

SURVIVAL MODELING FROM WHOLE SLIDE IMAGES VIA PATCH-LEVEL GRAPH CLUSTERING AND MIXTURE DENSITY EXPERTS

Ardhendu Sekhar, Vasu Soni, Keshav Aske, Garima Jain, Pranav Jeevan, Amit Sethi

Indian Institute of Technology Bombay

ABSTRACT

We present a modular framework for predicting cancer-specific survival from whole-slide pathology images (WSIs). The approach integrates four main components: (i) Quantile-Based Patch Filtering, which employs quantile-based thresholding to identify prognostically informative tissue regions; (ii) Graph Regularized Patch Clustering using k -NN graph to model phenotype-level heterogeneity through spatial–morphological coherence; (iii) Hierarchical Feature Aggregation for learning intra- and inter-cluster dependencies; and (iv) an Expert-Guided Mixture Density Modeling module to estimate complex survival distributions using Gaussian distributions. The proposed model achieves a concordance index of 0.653 ± 0.037 on TCGA-LUAD, 0.719 ± 0.011 on TCGA-KIRC, and 0.733 ± 0.037 on TCGA-BRCA, surpassing current state-of-the-art methods.

Index Terms— Survival Analysis, Whole-Slide Images, Attention, Mixture Density Expert, Deep Learning.

1. INTRODUCTION

Precise survival prediction from histopathology images is essential for personalized oncology, enabling effective treatment planning and risk assessment. Whole-slide images (WSIs) encapsulate detailed tissue morphology—covering tumor structure and its microenvironmental context—but their enormous resolution and absence of localized labels pose challenges for direct modeling. Consequently, patch-based multiple instance learning (MIL) has emerged as the prevailing approach, segmenting each slide into smaller tiles for weakly supervised analysis.

Although MIL has proven effective for cancer grading and subtyping, survival prediction further requires modeling long-range dependencies and subtle morphological cues across distant tissue regions. Traditional methods like the Cox proportional hazards model fail to capture such complex, non-linear relationships, while previous deep learning models often lack interpretability and spatial awareness.

To overcome these challenges, we introduce a unified framework comprising four key modules: (1) Quantile-Based Patch Filtering, which adaptively selects prognostically informative tissue regions via quantile thresholding; (2) Graph-Regularized Patch Clustering, designed to capture spatial–morphological coherence among relevant patches; (3) Hierarchical Feature Aggregation, enabling the learning of intra- and inter-cluster dependencies; and (4) an Expert-Guided Mixture Density Modeling component for estimating complex survival distributions. Collectively, these modules facilitate interpretable and accurate survival prediction by integrating spatial organization, phenotypic representation, and probabilistic outcome modeling.

2. RELATED WORK

Weakly supervised learning plays a pivotal role in WSI-based survival prediction, primarily utilizing multiple instance learning (MIL). Early approaches such as ABMIL [1], DSMIL [2], and CLAM [3] employed attention pooling to identify prognostic patches but neglected spatial dependencies. Graph-based models like PatchGCN [4] incorporated spatial relationships, while hierarchical transformer models such as HIPT [5], HGT [6], and TransMIL [7] captured multi-scale representations at significant computational cost. More recent multimodal frameworks—HiLa-X [8], PathoGen-X [9], and CoC [10]—combine histopathology with textual, genomics, or methylation data modalities, while SCMIL [11] models survival outcomes using a Normal distribution. Nevertheless, these methods lack explicit mechanisms to disentangle latent phenotypes or leverage structural coherence. Our expert-guided mixture density module bridges this gap by coupling phenotype-aware clustering with expert-based survival modeling, where specialized experts capture distinct prognostic cues and a gating network adaptively integrates their outputs for enhanced interpretability.

3. METHODOLOGY

Figure 1 presents an overview of the proposed model. Each Whole Slide Image (WSI) is partitioned

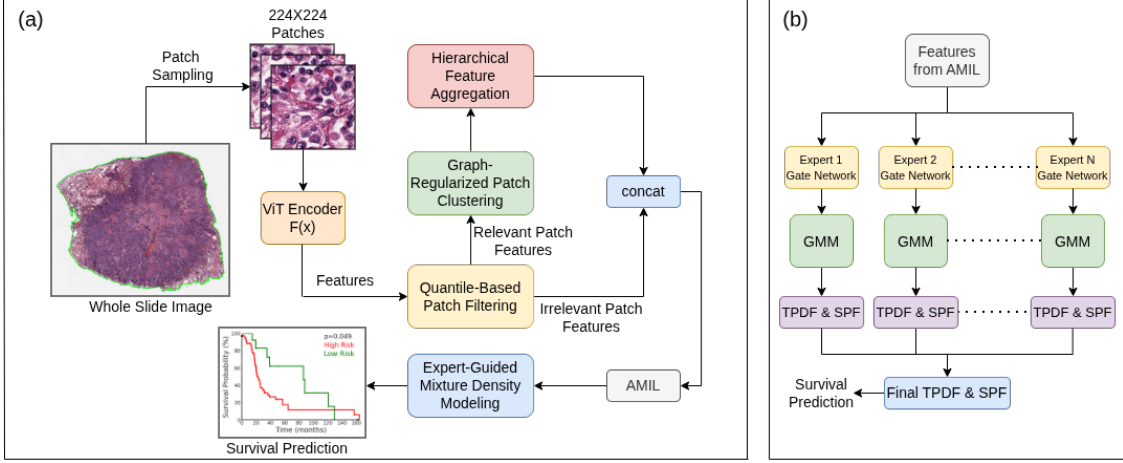


Fig. 1: (a) Proposed survival model. (b) Expert-guided Mixture Density Modeling block.

into non-overlapping 224×224 patches at the highest magnification ($40\times$). After excluding background and non-tissue areas, the remaining tissue patches are embedded using a histopathology foundation model[12] i.e. a Vision Transformer (ViT) feature extractor $F(x)$, pretrained with large-scale self-supervised learning[13] on diverse WSI datasets, generates the corresponding patch feature matrix:

$$\mathbf{P}_{\text{feat}} \in \mathbb{R}^{n \times d} \quad (1)$$

Here, n represents the total number of extracted patches, and d denotes the dimensionality of each feature vector.

The overall framework consists of four core modules: Quantile-Based Patch Filtering (QPF), Graph-Regularized Patch Clustering (GRPC), Hierarchical Feature Aggregation (HFA), and Expert-Guided Mixture Density Modeling (EGMDM).

3.1. Quantile-Based Patch Filtering (QPF)

To emphasize diagnostically significant regions, a learnable quantile-based Multi-Layer Perceptron (MLP) identifies task-relevant patches based on importance scores computed from model logits. For each WSI, a threshold τ_q corresponding to the q -quantile of logits is computed, preserving the top $(1 - q) \times 100\%$ of patches.

$$\mathcal{P}_{\text{sel}} = \{\mathbf{P}_i \mid \text{logit}_i > \tau_q\}, \quad \mathcal{P}_{\text{rem}} = \{\mathbf{P}_i \mid \text{logit}_i \leq \tau_q\}. \quad (2)$$

This dynamic filtering removes irrelevant patches, enabling subsequent modules to concentrate on semantically rich regions relevant to survival outcomes.

3.2. Graph-Regularized Patch Clustering (GRPC)

The selected patches $\mathcal{P}_{\text{sel}} \in \mathbb{R}^{m \times d}$ are clustered for both morphological and spatial consistency. Features and coordinates are normalized to a common scale, and

cosine similarity measures morphological relationships:

$$S_{\text{morph}}(i, j) = \frac{\langle \mathbf{P}_i, \mathbf{P}_j \rangle}{\|\mathbf{P}_i\| \|\mathbf{P}_j\|}, \quad (3)$$

Meanwhile, spatial similarity is measured using an exponential kernel applied to the Euclidean distances D_{ij} computed between the normalized patch coordinates:

$$S_{\text{spatial}}(i, j) = \exp\left(-\frac{D_{ij}}{\sigma_D}\right), \quad \text{where } \sigma_D = \text{std}(D) + \varepsilon. \quad (4)$$

A unified similarity matrix combines both cues:

$$S = \omega_{\text{morph}} S_{\text{morph}} + \omega_{\text{spatial}} S_{\text{spatial}} \quad (5)$$

Using the similarity matrix S , a k -nearest-neighbor (k -NN) graph is constructed, and GPU-accelerated K-Means guided by the graph topology clusters patches into G groups L_1, \dots, L_G . Each cluster reflects a specific tissue microenvironment—like tumor epithelium, stroma, or necrosis—providing a biologically meaningful and spatially consistent structure within the slide.

3.3. Hierarchical Feature Aggregation (HFA)

To model dependencies within clusters, a two-level attention mechanism is employed.

Intra-cluster attention. Each cluster L_i is processed using multi-head self-attention (MHSA) [14] to capture fine-grained local relationships among patches:

$$L'_i = \text{LayerNorm}(L_i + \text{MHSA}(L_i)). \quad (6)$$

This step improves contextual understanding within morphologically similar regions.

Inter-cluster attention. The refined clusters are condensed into representative embeddings.

$$R_i = \frac{1}{|L'_i|} \sum_{\mathbf{x} \in L'_i} \mathbf{x}, \quad (7)$$

which are subsequently passed through another MHSA layer to capture global relationships across regions:

$$R' = \text{LayerNorm}(R + \text{MHSA}(R)). \quad (8)$$

Intra-cluster features are concatenated as $\tilde{P} = \text{Concat}(L'_g)_{g=1}^G$. Averaging R' across clusters produces a broadcast descriptor R'_{exp} , expanded to match \tilde{P} and added residually to yield \hat{P} . Finally, \hat{P} is concatenated with unselected irrelevant patch features to form $\mathcal{P}_{\text{final}}$.

WSI-level aggregation. Slide-level representation is obtained through attention pooling as in AMIL [1].

$$\mathbf{z}_{\text{WSI}} = \sum_i \alpha_i \mathcal{P}_{\text{final},i}, \quad (9)$$

$$\alpha_i = \text{softmax}(W_a \tanh(W_h \mathcal{P}_{\text{final},i}^\top)),$$

where \mathbf{z}_{WSI} represents the aggregated prognostic feature of the WSI.

3.4. Expert-Guided Mixture Density Modeling (EGMDM)

The Expert-Guided Mixture Density Modeling block (Figure 1b) estimates continuous survival probabilities by modeling survival times, with each expert focusing on distinct WSI features \mathbf{z}_{WSI} . Following the mixture-of-experts paradigm [15] and SurvMDN [16], it constructs Gaussian mixtures to represent diverse survival patterns.

The survival time y corresponding to a whole slide image is modeled on its features \mathbf{z}_{WSI} , as illustrated in Figure 1b. Each expert e within the mixture outputs a Gaussian Mixture Model (GMM) over y :

$$p(y | \mathbf{z}_{\text{WSI}}, e) = \sum_{k=1}^K \lambda_k^{(e)}(\mathbf{z}_{\text{WSI}}) \mathcal{N}(y | \mu_k^{(e)}, \sigma_k^{(e)2}), \quad (10)$$

where each k component follows a Gaussian distribution with mean $\mu_k^{(e)}$ and standard deviation $\sigma_k^{(e)}$, while mixture weights $\lambda_k^{(e)}$ are computed via softmax over the K components. Learnable anchors $((P_\mu, P_\sigma) \in \mathbb{R}^K)$ represent shared mean and standard deviation vectors, linearly transformed for each expert:

$$\mu^{(e)} = W_\mu^{(e)} P_\mu, \quad \sigma^{(e)} = \text{softplus}(W_\sigma^{(e)} P_\sigma), \quad (11)$$

The survival time y is mapped to an unconstrained variable t via a softplus transformation $t = \log(1 + e^y)$, which ensures non-negativity in its Gaussian domain and produces the Jacobian factor $\frac{dy}{dt} = \frac{e^t}{e^t - 1}$. Finally, a gating network $G(\mathbf{z}_{\text{WSI}})$ assigns softmax probabilities across experts, yielding the overall survival probability functions:

$$\text{TPDF}(t | \mathbf{z}_{\text{WSI}}) = \frac{dy}{dt} \sum_{e,k} G_e(\mathbf{z}_{\text{WSI}}) \lambda_k^{(e)} \times \mathcal{N}(g^{-1}(t) | \mu_k^{(e)}, \sigma_k^{(e)2}) \quad (12)$$

$$\text{SPF}(t | \mathbf{z}_{\text{WSI}}) = 1 - \sum_{e,k} G_e(\mathbf{z}_{\text{WSI}}) \lambda_k^{(e)} \Phi\left(\frac{g^{-1}(t) - \mu_k^{(e)}}{\sigma_k^{(e)}}\right) \quad (13)$$

where Φ is derived by integrating \mathcal{N} , TPDF denotes the transformed probability density of death, and SPF represents the survival probability at time t .

3.5. Training Objective and Regularization

The model is trained using a negative log-likelihood loss (\mathcal{L}_{NLL}) that accounts for both censored ($c = 0$ i.e. event not yet occurred) and uncensored ($c = 1$, i.e. event occurred) cases. Given an observed time t_d and censoring indicator $c \in \{0, 1\}$,

$$\mathcal{L}_{\text{NLL}} = -c \log(\text{TPDF}(t_d | \mathbf{z}_{\text{WSI}})) - (1 - c) \log(\text{SPF}(t_d | \mathbf{z}_{\text{WSI}})) \quad (14)$$

To promote interpretability and specialization, a gating entropy loss (\mathcal{L}_{ent}) is introduced for diverse expert usage.

$$\mathcal{L}_{\text{ent}} = -\sum_e G_e(\mathbf{z}_{\text{WSI}}) \log(G_e(\mathbf{z}_{\text{WSI}})) \quad (15)$$

The total loss is:

$$\mathcal{L}_{\text{total}} = \mathcal{L}_{\text{NLL}} + \lambda_{\text{ent}} \mathcal{L}_{\text{ent}}. \quad (16)$$

4. EXPERIMENTAL SETUP

4.1. Datasets

We assess the proposed model on three TCGA cohorts: Lung Adenocarcinoma (LUAD; 459 WSIs), Kidney Renal Clear Cell Carcinoma (KIRC; 509 WSIs), and Breast Invasive Carcinoma (BRCA; 956 WSIs) [18]. Each cohort comprises WSIs annotated with overall survival time, recorded in months from diagnosis to death (uncensored, $c = 1$) or until the last follow-up (censored, $c = 0$).

4.2. Training Configuration

The quantile of patch filtering module is fixed at $q=0.25$, selecting the top 75% of patches by their logits. The k-NN graph built on similarity matrix S , connects each node to 10 neighbors, clustering patch indices into G groups of 64 each and those corresponding patches are processed by an 8-head MHSA in the HFA module. The Expert-Guided Mixture Density block employs five experts, each modeling a $K = 100$ Gaussian mixture. Training runs for 20 epochs with Adam ($\text{lr } 2 \times 10^{-4}$, weight decay 1×10^{-3}), batch size 1. Performance is reported as mean \pm std of the Time-Dependent Concordance Index (TDC) [16] over 5-fold cross-validation on an NVIDIA A6000 GPU.

5. RESULTS AND ANALYSIS

5.1. Quantitative Results

Table 1a presents the model's performance across all datasets. Our framework consistently attains the highest

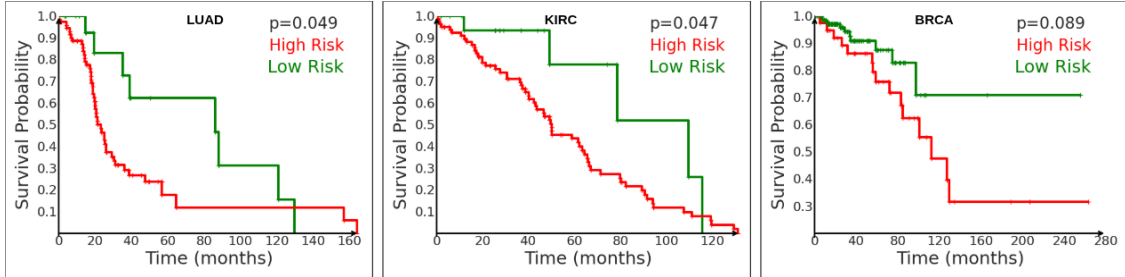


Fig. 2: Kaplan–Meier survival plots illustrating distinct high and low-risk group separation across TCGA cohorts.

Table 1: Left: TCGA results (TDC, higher is better). Right: Ablations on q in QPF, GRPC, HFA and e in EGMDM. Best TDC values in **bold**.

(a) TCGA results. Modality: I=image, G=genomic, M=methylation, L=language prompt.

(b) Ablations.

Method	Modality	LUAD	KIRC	BRCA	MEAN	Variant	LUAD	KIRC	BRCA
AMIL [1]	I	0.624 ± 0.038	0.638 ± 0.065	0.654 ± 0.013	0.639	$q=0.5$ in QPF	0.634±0.022	0.700±0.052	0.720±0.046
CLAM [3]	I	0.605 ± 0.051	0.676 ± 0.032	0.632 ± 0.045	0.638	$q=0.75$ in QPF	0.625±0.041	0.690±0.037	0.710±0.019
DSMIL [2]	I	0.593 ± 0.065	0.655 ± 0.031	0.618 ± 0.021	0.622	w/o QPF	0.626±0.053	0.691±0.065	0.711±0.027
TransMIL [7]	I	0.545 ± 0.037	0.632 ± 0.036	0.591 ± 0.013	0.589	w/o GRPC, HFA	0.621±0.046	0.685±0.050	0.705±0.011
SetMIL [17]	I	0.620 ± 0.027	0.694 ± 0.052	0.635 ± 0.027	0.650	$e=1$ in EGMDM	0.638±0.049	0.698±0.013	0.717±0.057
PatchGCN [4]	I	0.587 ± 0.019	0.675 ± 0.045	0.582 ± 0.037	0.615	Ours (All)	0.653±0.037	0.719±0.011	0.733±0.037
HIPT [5]	I	0.549 ± 0.025	0.640 ± 0.037	0.625 ± 0.046	0.605				
HGT [6]	I	0.607 ± 0.058	0.648 ± 0.018	0.638 ± 0.022	0.631				
SCMIL [11]	I	0.622 ± 0.015	0.688 ± 0.037	0.674 ± 0.048	0.661				
PathoGen-X [9]	I+G	0.620 ± 0.008	— —	0.670 ± 0.020	0.645				
CoC [10]	I+M	— —	0.709 ± 0.048	0.654 ± 0.036	0.682				
HiLa [8]	I+L	0.643 ± 0.055	— —	0.659 ± 0.044	0.651				
Ours	I	0.653 ± 0.037	0.719 ± 0.011	0.733 ± 0.037	0.700				

mean TDC, reflecting superior discrimination and calibration. Histopathology-based multiple instance learning (MIL) models—AMIL [1], CLAM [3], DSMIL [2], TransMIL [7], and SetMIL [17]—served as the backbones for the expert-guided mixture density module, with results reported for comparison. Survival-oriented MIL approaches such as HIPT [5], Patch-GCN [9], HGT [6], and SCMIL [11] act as benchmarks. As multimodal frameworks [9, 10, 8] lack open-source implementations, their reported results are drawn from the original publications. By combining quantile-based patch filtering, graph clustering, hierarchical aggregation, and expert-guided mixture density modeling—each expert capturing distinct morphological or contextual cues—our approach effectively identifies survival-relevant regions and achieves state-of-the-art results across all datasets, even surpassing multimodal counterparts while using only histopathology data.

5.2. Ablation Studies and Interpretability

Ablation experiments evaluated the effects of Quantile-Gated Patch Filtering, Graph-Regularized Patch Clustering, Hierarchical Feature Aggregation, and Expert-Guided Mixture Density Modeling (Table 1b). A quantile of $q=0.25$ offered the best trade-off, retaining prognostic regions while suppressing noise. Removing any module reduced TDC, confirming their complementary

roles in denoising and spatial reasoning. Single-expert models underperformed, whereas five experts improved results, highlighting the value of multi-expert modeling. For interpretability, patients were stratified into high- and low-risk groups using predicted survival scores. Kaplan–Meier curves (Fig. 2) showed clear separation (log-rank $p=0.049$ LUAD, $p=0.047$ KIRC, $p=0.089$ BRCA), validating prognostic relevance and regional localization.

6. CONCLUSION

We introduced a unified framework for WSI-based survival prediction that combines quantile-regularized patch filtering, graph-based patch clustering, hierarchical feature aggregation, and expert-guided mixture density modeling. By capturing local–global tissue dependencies through clustered attention and modeling survival distributions using mixture experts, the approach enhances both calibration and discrimination. Experiments on TCGA-LUAD, TCGA-KIRC, and TCGA-BRCA demonstrate consistent improvements in time-dependent concordance compared to pathology-based and multimodal baselines. Future directions include extending the framework to multimodal and uncertainty-aware patient-level survival prediction for improved clinical robustness.

7. COMPLIANCE WITH ETHICAL STANDARDS

This study employed publicly available human data from [18]; thus, no separate ethical approval was required under the open-access license.

8. ACKNOWLEDGMENTS

This study’s findings are based on data from the TCGA Research Network [18].

9. REFERENCES

- [1] Maximilian Ilse, Jakub M. Tomczak, and Max Welling, “Attention-based deep multiple instance learning,” 2018.
- [2] Bin Li, Yin Li, and Kevin W. Eliceiri, “Dual-stream multiple instance learning network for whole slide image classification with self-supervised contrastive learning,” 2021.
- [3] Ming Y. Lu, Drew F. K. Williamson, Tiffany Y. Chen, Richard J. Chen, Matteo Barbieri, and Faisal Mahmood, “Data efficient and weakly supervised computational pathology on whole slide images,” 2020.
- [4] Richard J. Chen, Ming Y. Lu, Muhammad Shaban, Chengkuan Chen, Tiffany Y. Chen, Drew F. K. Williamson, and Faisal Mahmood, “Whole slide images are 2d point clouds: Context-aware survival prediction using patch-based graph convolutional networks,” 2021.
- [5] Richard J. Chen, Chengkuan Chen, Yicong Li, Tiffany Y. Chen, Andrew D. Trister, Rahul G. Krishnan, and Faisal Mahmood, “Scaling vision transformers to gigapixel images via hierarchical self-supervised learning,” 2022.
- [6] “Multi-scope analysis driven hierarchical graph transformer for whole slide image based cancer survival prediction,” in *Medical Image Computing and Computer Assisted Intervention – MICCAI 2023*, Cham, 2023, pp. 745–754, Springer Nature Switzerland.
- [7] Zhuchen Shao, Hao Bian, Yang Chen, Yifeng Wang, Jian Zhang, Xiangyang Ji, and Yongbing Zhang, “Transmil: Transformer based correlated multiple instance learning for whole slide image classification,” 2021.
- [8] Jiaqi Cui, Lu Wen, Yuchen Fei, Bo Liu, Luping Zhou, Dinggang Shen, and Yan Wang, “HiLa: Hierarchical Vision-Language Collaboration for Cancer Survival Prediction,” in *Medical Image Computing and Computer Assisted Intervention – MICCAI 2025*, October 2025, vol. LNCS 15964, pp. 240 – 250, Springer Nature Switzerland.
- [9] Akhila Krishna, Nikhil Cherian Kurian, Abhijeet Patil, Amruta Parulekar, Pranav Jeevan P, and Amit Sethi, “Pathogen-x: A cross-modal genomic feature trans-align network for enhanced survival prediction from histopathology images,” in *2025 IEEE 22nd International Symposium on Biomedical Imaging (ISBI)*, 2025, pp. 1–4.
- [10] Haipeng Zhou, Sicheng Yang, Sihan Yang, Jing Qin, Lei Chen, and Lei Zhu, “CoC: Chain-of-Cancer based on Cross-Modal Autoregressive Traction for Survival Prediction,” in *Medical Image Computing and Computer Assisted Intervention – MICCAI 2025*, October 2025, vol. LNCS 15974, pp. 85 – 94, Springer Nature Switzerland.
- [11] Zekang Yang, Hong Liu, and Xiangdong Wang, *SCMIL: Sparse Context-Aware Multiple Instance Learning for Predicting Cancer Survival Probability Distribution in Whole Slide Images*, p. 448–458, Springer Nature Switzerland, 2024.
- [12] Mingu Kang, Heon Song, Seonwook Park, Donggeun Yoo, and Sérgio Pereira, “Benchmarking self-supervised learning on diverse pathology datasets,” 2023.
- [13] Xinlei Chen, Saining Xie, and Kaiming He, “An empirical study of training self-supervised vision transformers,” 2021.
- [14] A. et al. Vaswani, “Attention is all you need,” in *Advances in Neural Information Processing Systems*, 2017.
- [15] Christopher M. Bishop, *Pattern Recognition and Machine Learning*, Springer, New York, 2006.
- [16] Xintian Han, Mark Goldstein, and Rajesh Ranganath, “Survival mixture density networks,” 2022.
- [17] Yu Zhao, Zhenyu Lin, Kai Sun, Yidan Zhang, Junzhou Huang, Liansheng Wang, and Jianhua Yao, “Setmil: Spatial encoding transformer-based multiple instance learning for pathological image analysis,” in *Proc. MICCAI*, 2022, pp. 66–76.
- [18] TCGA Research Network, “The cancer genome atlas pan-cancer analysis project,” *Nature Genetics*, vol. 45, no. 10, pp. 1113–1120, 2013.